Available online at www.sciencedirect.com

ScienceDirect

IFAC PapersOnline CONFERENCE PAPER ARCHIVE

IFAC PapersOnLine 56-3 (2023) 343–348

A nonlinear fractional-order dynamical framework for state of charge estimation of $LiFePO_4$ batteries in electric vehicles

Manashita Borah[1,2,*]. Scott Moura[1]. Dylan Kato[1]. Jaewoong Lee[1]**

[1]*Energy, Controls and Application Laboratory, Department of Civil and Environmental Engineering, University of California, Berkeley, USA, 94720*

*(e-mail: *manashitaborah@gmail.com, *manashitaborah@berkeley.edu, ** smoura@berkeley.edu)*

[2]*Department of Electrical Engineering, Tezpur University, Assam, India, 784028*

Abstract: An efficient state of charge (SOC) estimation for $LiFePO_4$ batteries in electric vehicles (EVs) has been an open problem so far, largely due to its non-measurable nature. This paper tackles this problem by presenting a fractional-order (FO) dynamical framework to unravel and understand the inherent dynamics of the $LiFePO_4$ battery which leads to an improved estimation of SOC. First, a FO model (FOM) is proposed where the parameters are introduced as nonlinear functionalities of SOC. It has been observed that the FO defined as a nonlinear function of SOC is crucial in identifying its progression during the weakly measurable flat, open circuit curve of the battery; a property the integer order models (IOMs) fail to capture. Second, a fractional order estimator (FOE) is designed incorporating the SOC based nonlinearities of the model parameters. The FO derivative being a memory-based operator improves estimation as it can store historical information of the speed profiles of the EV. The proposed framework of nonlinear FOM and FOE design is validated through both simulation and experimental results. Precise estimation of the battery parameters using the proposed framework can be applied to protect the battery management system, mitigate overcharge or discharge, prevent hazardous accidents, and enhance battery life, eventually leading to an energy-efficient mode of green transportation.

Copyright © 2023 The Authors. This is an open access article under the CC BY-NC-ND license (https://creativecommons.org/licenses/by-nc-nd/4.0/)

Keywords: fractional-order, Lithium-ion batteries, electric vehicles, state of charge estimation, green transportation

1. INTRODUCTION

In this era of developing climate consciousness and devising new and improved technology solutions to attain a sustainable environment, electric vehicles play a promising role. Lithium-ion batteries (LIBs) are the leading energy storage technology for the current as well as next generation transportation systems based on clean, green, and sustainable energy solutions. The existing LIBs however still suffer from technical challenges of safety, reliability, cost, weight and lifespan, lack of real-time measurements and parametric uncertainties (Dey et al., 2015).

1.1 A brief recent survey

Accurate estimation of SOC of Lithium Ferrous Phosphate (LFP/ $LiFePO_4$) batteries has long been an open problem. A recent industrial survey discloses a global trend of manufacturers of EVs shifting to LFP batteries for standard range vehicles from the existing Nickel Manganese Cobalt (NMC) batteries that have been predominantly used in high end EVs so far (Klender, 2021). The current bottlenecks of NMC are its safety hazard due to the thermal runaway, scarcity of raw materials of Nickel and Cobalt, short lifespan, and high cost (Volta, 2021). Though LFP overcomes these limitations, however the transition to LFPs in EVs is still in nascent stage as the long-standing challenge of error-free estimation of SOC, largely due to its limited observability, is unsolved. The drawbacks in the existing battery parameter estimation research are as follows:

i. limited capture of battery dynamics through IOMs,

ii. utilization of a fully linearized model where the dependence of the parameters on SOC is ignored,

iii. failure of conventional methods of observer design like extended Kalman filter (EKF) to provide an optimal estimate due to the internal linearization (Dey et al., 2014), data-driven methods on the other hand require huge amount of data for training, apart from being black box models (Liu, et al., 2023; Yao et al., 2023).

In practical scenarios, one of the short comings in an IO equivalent circuit model (ECM) is that the capacitors and inductors may not mimic the system behaviour at an in-depth capacity, especially, when the relationship between voltage and current is not always an integral derivative. These non-ideal relationships are captured by a FO capacitor or an FO inductor called a fractor, whose impedance is termed as fractance, the circuit of which is successfully realized in (Adhikary et al., 2016). FOM circuits have been found to deliver improved results in various real life applications as in secure communication and multistable hypogenetic systems (Borah et al., 2017; Borah et al., 2018). Experiments on frequency spectrum of LFP cells obtained from

2405-8963 Copyright © 2023 The Authors. This is an open access article under the CC BY-NC-ND license.
Peer review under responsibility of International Federation of Automatic Control.
10.1016/j.ifacol.2023.12.048

electrochemical impedance spectroscopy (EIS) reveal that an FOM can acquire the dynamics of mid-frequency region such as charge transfer reaction and double layer effects and that of low frequency region as solid phase diffusion of the battery better than the corresponding IOMs (Nasser-Eddine et al., 2019). Fractional-order calculus has been extended to data driven methods such as FO gradient based recurrent neural networks for SOC estimation of LIBs in (Wang et al., 2022), where it has also been reported that FO constraints can stabilise the output and reduce its noise. Recently, an FO framework has been developed to co-estimate SOC of a hybrid energy storage system, resulting in an improved and faster convergence (Li et al., 2023), however the dependence of the circuit parameters on the SOC was ignored. An observer for SOC estimation of LFP battery using fractional calculus is proposed in (Rao et al., 2021) nevertheless, the FOM validation is not performed and the proposed observer is a low gain linear observer that may not guarantee convergence. The FOMs can closely capture the real dynamics of a physical system owing to their following extraordinary advantages (Borah et al., 2022; Chen et al.,2023):

i. FO derivative being a non-local operator has the capacity to store infinite memory of the past values calculated until the present time, unlike IO derivative which is a memory less operator,
ii. FO derivative being a non-ideal operator can incorporate non-integer values, unlike IO derivatives,
iii. the additional FO parameter gives more flexibility and a larger stability region.

1.2 Novelty and contribution

This paper attempts to address the open problem of SOC estimation of LFP batteries by presenting a framework of FO modelling and estimation as in the following.

i. A FO framework is proposed where the FO operator along with the circuit parameters in the LFP battery model are defined as nonlinear functions of SOC, and validated experimentally. The authors claim novelty in this innovative approach, as it not only improves model accuracy but also adds mathematical dependencies between measured voltage and SOC beyond the flat open circuit curve; a critical and partially understood dynamics of LFP battery. In a fresh attempt, our work validates the above nonlinear functionalities of parameters with SOC with experimental evidence in the frequency domain; a contribution not made so far in the existing literature to the best of the authors' knowledge. This novelty helps to understand the inter correlation and progression of the unknown LFP battery physics as the SOC varies during dynamic operating conditions. Besides, the FOM also contributes in capturing the dynamics of solid-phase diffusion and charge transfer reaction dynamics, which otherwise remain unobserved in an IOM.
ii. A nonlinear observer is designed using the FO Lyapunov stability criterion to estimate the SOC performance, incorporating the SOC based nonlinearities of the model parameters. It is found to generate improved results in comparison to existing FO estimation techniques for LFP.

The paper is organized as follows. A brief introduction and contribution of this work is highlighted in Section 1. The first step of the FO dynamical framework with the proposed FOM and its parameter identification are stated in Section 2. Section 3 details the nonlinear observer design for SOC estimation. The results are validated and discussed in Section 4 and the paper is finally concluded in Section 5.

2. PROPOSED FRACTIONAL-ORDER MODEL

This section presents the fundamentals of fractional calculus followed by the first step of the proposed framework, i.e. design of the FOM.

2.1 Preliminaries of fractional calculus

The Caputo fractional derivative of order α of a continuous function *f(t)* is defined as in (1) (Monje et al., 2010).

$$D_t^{\alpha} f(t) = \frac{d^{\alpha} f(t)}{dt^{\alpha}} = \begin{cases} \frac{1}{\Gamma(m-\alpha)} \int_0^t \frac{f^{(m)}(\tau)}{(t-\tau)^{\alpha-m+1}} d\tau, & m-1 < \alpha < m,\ m \in \mathbb{N} \\ \frac{d^m}{dt^m} f(t), & \alpha = m \end{cases} \quad (1)$$

The Laplace transform of the Caputo fractional derivative is:

$$L\left\{\frac{d^{\alpha} f(t)}{dt^{\alpha}}\right\} = s^{\alpha} L\{f(t)\} - \sum_{k=0}^{m-1} s^{\alpha-k-1} f^{(k)}(0) \quad (2)$$

Theorem 1 (Monje et al., 2010**)**: The equilibrium points of a commensurate FO nonlinear dynamical system (FONLS) are asymptotically stable if for all the eigenvalues $\lambda_i, (i = 1, 2, \ldots, n)$ of the Jacobian matrix $J = {\partial f}/{\partial x}$, where $f = [f_1, f_2, \ldots, f_n]^T$, evaluated at the equilibrium point, satisfy the condition: $|arg(eig(J))| = |arg(\lambda_i)| > \alpha\pi/2, i = 1,2,\ldots,n$.

Lemma 1: (Aguila-Camacho, Duarte-Mermoud & Gallegos, 2014) If $x(t) \in \mathbb{R}$ is a continuous and derivable function, then, for any time instant $t \geq 0$,

$$\frac{1}{2} D^{\alpha} x^2(t) \leq x(t) D^{\alpha} x(t), \qquad \forall \alpha \in (0,1]$$

where $D^{\alpha} x(t)$ is the Caputo fractional derivative of $x(t)$ of FO α. Based on the above preliminaries, the FO dynamical framework is presented in the following sections

2.2 FO Modelling and Parameter identification

The generalized form of FONLS is presented in (3) and (4),

$$D^{\alpha} x(t) = A(x)x(t) + g(x,u) \quad (3)$$

$$y = Cx \quad (4)$$

where x is the vector containing the unmeasurable states, u and y are measurable input and output vectors, $A(x)$ represents the nonlinear function in x and $\alpha = \{\alpha_1, \alpha_2, \ldots, \alpha_n\}$ is the FO parameter vector such that $\alpha \in (0,1]$.

The first step of the framework is presented in Fig. 1.

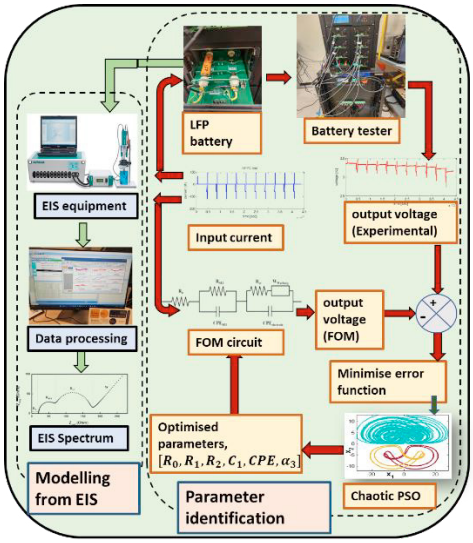

Fig. 1. Framework of FO modelling and identification

The FOM of a battery is conceptually built from EIS, where the impedance is calculated from the terminal voltage in response to a small input alternating current. The Nyquist plot of the impedance spectrum is then divided in three frequency regions: low (solid phase diffusion), mid (charge transfer reaction, double layer effect) and high (ohmic polarization). The low frequency region in the Nyquist plot obtained from the EIS experiment is modelled using a FO element called the constant phase element (CPE). It can attain non-integral values unlike a conventional capacitor and thus model the fractional solid phase diffusion dynamics better. The resultant FO-ECM is depicted in Fig.2, where V_{oc} and V_t are open circuit and terminal voltages of the battery, respectively.

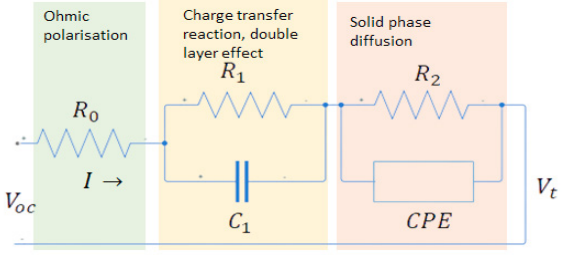

Fig. 2 Proposed FOM of the LFP battery, depicting the dynamics during low, high and mid frequency ranges

The FO-ECM in Fig. 2 results in an FONLS from (3)-(4) as in (5) and (6)

$$\begin{cases} D^{\alpha_1}x_1(t) = -\dfrac{u(t)}{Q} \\ D^{\alpha_2}x_2(t) = -\dfrac{1}{R_1(x_1)C_1(x_1)}x_2(t) + \dfrac{1}{C_1(x_1)}u(t) \\ D^{\alpha_3}x_3(t) = -\dfrac{1}{R_2(x_1)CPE(x_1)}x_3(t) + \dfrac{1}{R_2(x_1)CPE(x_1)}u(t) \\ D^{\alpha_4}x_4(t) = -\gamma\{x_4(t) - V_t\} \end{cases} \quad (5)$$

$$\text{output voltage } y = Cx = [0\ 0\ 0\ 1]\ x_4 \quad (6)$$

where, $V_t = V_{oc}(x_1) - x_2(t) - x_3(t) - R_0(x_1)u(t)$, and $\alpha = \{\alpha_1, \alpha_2, \alpha_3, \alpha_4\} = \{1,1,\alpha_3,1\}$. The state vector $x = [x_1 \quad x_2 \quad x_3 \quad x_4]^T$ is such that $x_1 = SOC$, x_2 is the voltage across the R_1C_1 pair, x_3 is the voltage across the R_2CPE pair and x_4 is the output terminal voltage, V_t at equilibrium. x_1, x_2 and x_3 are non-measurable states and x_4 is a measurable state at equilibrium. Q is the battery nominal capacity, u is the input current I which is positive for discharging and negative for charging operations.

Once the frequency domain experiment is conducted, the parameter identification of the above FO-ECM in (5) and (6) is carried out using global optimization techniques. The LFP battery is subjected to an Hybrid Pulse Power Characterization (HPPC) or any pulse load current for each 10% drop of SOC and allowed to rest for 10 minutes. It is repeated until the lower cut-off voltage of the battery is achieved. The V_t at the resting period gives the V_{oc} and the corresponding relationship of the $V_{oc} - SOC$ curve, i.e. $V_{oc}(x_1)$ is derived. Now the optimization problem is framed such that the error between the experimental output terminal voltage and the model output voltage is minimized as given in (7).

$$\min e(\hat{\theta}) = \frac{1}{q}\left[\sum_{k=1}^{q}(V_{t(exp)}(t_k) - V_{t(FOM)}(t_k))^2\right]^{\frac{1}{2}} \quad (7)$$

In (7), $V_{t(exp)}(t_k)$ and $V_{t(FOM)}(t_k)$ are the experimental terminal voltage and the FOM terminal voltage obtained at k^{th} sample and $\theta = [R_0, R_1, R_2, C_1, CPE, \alpha_3]$ represents the set of parameters to be optimized. The parameters are identified once the cost function converges and likewise the parameter identification is performed for varying values of SOC. The identified parameters are thus nonlinear functions dependent on SOC. Following the parameter identification, we proceed to design an estimator/ observer to estimate the unmeasurable state, SOC in the forthcoming section.

3. DESIGN OF OBSERVER

The second step of the framework is the design of a nonlinear observer in the FO sense presented in this section.

Let, $b = \frac{1}{Q}$, $k_1(x_1) = \frac{1}{R_1(x_1)C_1(x_1)}$, $k_2(x_1) = \frac{1}{R_2(x_1)CPE(x_1)}$, $k_3(x_1) = V_{oc}(x_1)$, $p_1(x_1) = \frac{1}{C_1(x_1)}$, $p_2(x_1) = \frac{1}{CPE(x_1)}$, $p_3(x_1) = R_0(x_1)$ so that (5) and (6) simplify to (8) and (9).

$$\begin{cases} D^{\alpha_1}x_1 = -bu \\ D^{\alpha_2}x_2 = -k_1(x_1)x_2 + p_1(x_1)u \\ D^{\alpha_3}x_3 = -k_2(x_1)x_3 + p_2(x_1)u \\ D^{\alpha_4}x_4 = -\gamma\{x_4 - V_{oc}(x_1) + x_2 + x_3 + p_3(x_1)u\} \end{cases} \quad (8)$$

$$y = x_4 \quad (9)$$

The general form of FO observed model is given by,

$$D^{\alpha}\hat{x}(t) = A(\hat{x})\hat{x}(t) + g(\hat{x}, u) + L(y - \hat{y}) \quad (10)$$

$$\hat{y} = C\hat{x}(t) \quad (11)$$

where $\hat{x}(t)$is the estimation of $x(t)$, $L = [l_1 \quad l_2 \quad l_3 \quad l_4]^T$ is the observer gain matrix to be designed.

The observed FO battery model is presented in (12).

$$\begin{cases} D^{\alpha_1}\hat{x}_1 = -bu + l_1(x_4 - \hat{x}_4) \\ D^{\alpha_2}\hat{x}_2 = -k_1^0(\hat{x}_1)\hat{x}_2 + p_1^0(\hat{x}_1)u + l_2(x_4 - \hat{x}_4) \\ D^{\alpha_3}\hat{x}_3 = -k_2^0(\hat{x}_1)\hat{x}_3 + p_2^0(\hat{x}_1)u + l_3(x_4 - \hat{x}_4) \\ D^{\alpha_4}\hat{x}_4 = \gamma\{k_3^0(\hat{x}_1) - \hat{x}_2 - \hat{x}_3 - p_3^0(\hat{x}_1)u + l_4(x_4 - \hat{x}_4)\} \end{cases} \quad (12)$$

Here in (9), $k_i^0(\cdot)$ and $p_i^0(\cdot)$ are the nominal representations of $k_i(\cdot)$ and $p_i(\cdot)$ and are chosen as locally Lipschitz and bounded defined as follows $k_i^0(\cdot) \leq -m_i$, $1 \leq i \leq 3$.

The estimation error is defined as, $e = x - \hat{x}$ and the error dynamics is defined in (13).

$$\begin{cases} D^{\alpha_1}e_1 = -l_1 e_4 \\ D^{\alpha_2}e_2 = -k_1(x_1)x_2 + k_1^0(\hat{x}_1)\hat{x}_2 + \{p_1(x_1) - p_1^0(\hat{x}_1)\}u - l_2 e_4 \\ D^{\alpha_3}e_3 = -k_2(x_1)x_3 + k_2^0(\hat{x}_1)\hat{x}_3 + \{p_2(x_1) - p_2^0(\hat{x}_1)\}u - l_3 e_4 \\ D^{\alpha_4}e_4 = k_3(x_1) - k_3^0(\hat{x}_1) + e_2 + e_3 + \{p_3(x_1) - p_3^0(\hat{x}_1)\}u - l_4 e_4 \end{cases} \quad (13)$$

Further mathematical calculation reveals

$$-k_1(x_1)x_2 + k_1^0(\hat{x}_1)\hat{x}_2 = -k_1^0(\hat{x}_1)e_2 + \{k_1^0(\hat{x}_1) - k_1(x_1)\}x_2$$

and

$$-k_2(x_1)x_3 + k_2^0(\hat{x}_1)\hat{x}_3 = -k_2^0(\hat{x}_1)e_3 + \{k_2^0(\hat{x}_1) - k_2(x_1)\}x_3$$

which can be substituted in (13).

The boundedness of the following function in (14) are defined as,

$$\begin{aligned} &\|\{k_1^0(\hat{x}_1) - k_1(x_1)\}x_2\| + \|\{p_1(x_1) - p_1^0(\hat{x}_1)\}u\| \leq M_1 \\ &\|\{k_2^0(\hat{x}_1) - k_2(x_1)\}x_3\| + \|\{p_2(x_1) - p_2^0(\hat{x}_1)\}u\| \leq M_2 \\ &\|k_3(x_1) - k_3^0(\hat{x}_1)\| + \|\{p_3(x_1) - p_3^0(\hat{x}_1)\}u\| \leq M_3 \end{aligned} \quad (14)$$

where M_i $1 \leq i \leq 3$ are all positive bounded constants.

The Lyapunov function is chosen as a positive definite function as in (15).

$$V(e) = \frac{1}{2}(e_1^2 + e_2^2 + e_3^2 + e_4^2) \quad (15)$$

The error dynamics in (16) is obtained using Caputo fractional derivative (1) and lemma 1 in $V(e)$

$$\begin{aligned} D^{\alpha}V(e) &\leq e_1 D^{\alpha}(e_1) + e_2 D^{\alpha}(e_2) + e_3 D^{\alpha}(e_3) + e_4 D^{\alpha}(e_4) \\ &\leq e_1(-l_1 e_4) + e_2(-m_1 e_2 + M_1 - l_2 e_4) \\ &\quad + e_3(-m_2 e_3 + M_2 - l_3 e_4) + e_4(M_3 + e_2 \\ &\quad + e_3 - l_4 e_4) \\ &\leq -m_1 {e_2}^2 - m_2 {e_3}^2 - l_4 {e_4}^2 - l_2 e_4 e_2 - l_3 e_4 e_3 + \\ &e_2 e_4 + e_4 e_3 + M_1 e_2 + M_2 e_3 + M_3 e_4 \end{aligned} \quad (16)$$

The observer gains are chosen such that $D^{\alpha}V(e) \to 0$ as time $t \to \infty$.

4. EXPERIMENTAL RESULTS AND DISCUSSIONS

The experimental validations of the simulation results are discussed in the following two subsections.

4.1 Step 1 of the framework: parameter identification of FOM

This subsection implements the first step of the FO framework discussed in Section 2.2. First, we utilize EIS experimental data to demonstrate how an FOM more accurately captures the frequency response relative to an IOM. Then, we identify the FOM parameters from drive cycle data.

The laboratory set up for the EIS experiment consist of a Gamry1010E instrument which has a maximum applied current of ±1 A, maximum applied potential of ±12 V and a frequency range of 10 μHz - 2 MHz It is interfaced with a workstation that processes the data. EIS experiments are conducted on a fresh 18650 LFP cell of 3.3 V nominal voltage, 1.2 Ah capacity. The input to the EIS is an alternating current of 0.1 A and the frequency spectrum is varied from 0.01 Hz to 100 kHz at 25^0 C. The Nyquist plot derived from the EIS is plotted in blue and the fitted model (using the circuit illustrated previously in Fig. 2), in red in Fig. 3. It is seen that the FOM fits the experimental frequency data better by capturing the solid phase diffusion as shown in Fig. 3b, than that by an IOM, in Fig. 3a) where the CPE is replaced by an integral capacitor.

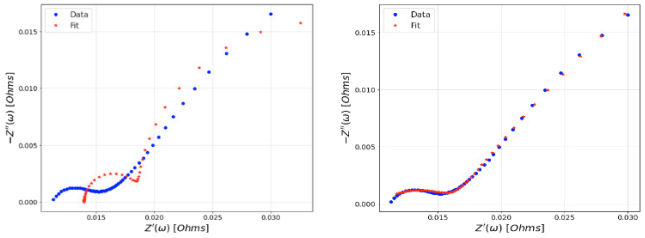

a) IOM b) FOM

Fig. 3. Nyquist plot spectrum from EIS experiment (blue) fitted by the equivalent circuit models (red)

The input current of the EIS experiment in the frequency domain has a constant profile, whereas the current profiles in real life scenarios are highly fluctuating. This calls for a parameter identification in the time domain using current profiles under actual operating conditions. The experimental setup is shown in Fig. 4 which displays an Arbin laboratory battery tester (LBT) with a channel voltage range of 0-10V, maximum channel current of 10A divided into four ranges of 10A / 500 mA/ 20 mA/ 1mA and eight number of channels.

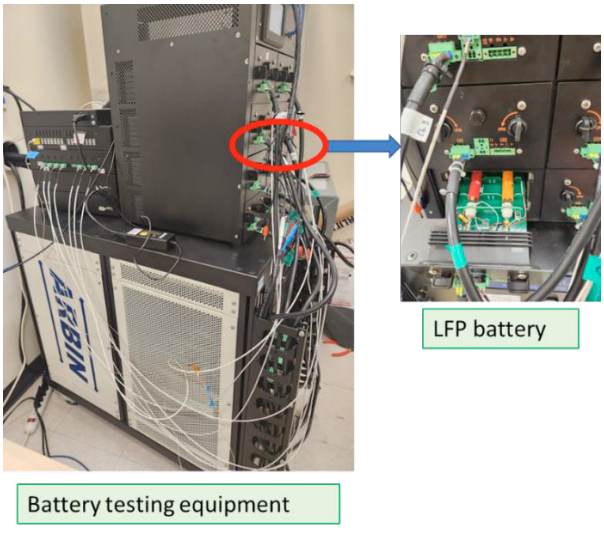

Fig.4 Experimental set up of battery tester

An Urban Dynamometer Driving Schedule (UDDS) profile is taken for the purpose as shown in Fig 5 and the parameters are identified such that each parameter is a nonlinear function of

SOC. In order to mitigate the impact of hysteresis on the battery dynamics, V_{oc} is taken as the average of the charging and discharging current profiles.

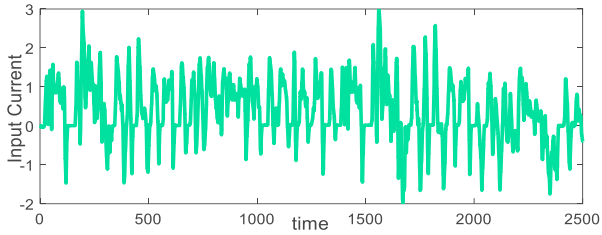

Fig.5 UDDS input current profile

The parameter identification is carried out using chaos based PSO (Duan et al., 2022), where the cost function is optimized with respect to three indices: position, speed and fitness. A peculiar characteristic of chaotic trajectories is that they never repeat their paths or intersect. This property of chaos introduces a randomness in the PSO algorithm which facilitates the particles to explore previously unexplored regions of the solution space, escape local optima, and thereby attain global optima in terms of potentially finding better solutions (Tian, 2017). This is the reason behind using chaos-based PSO for parameter identification, as opposed to gradient-based optimizers, for example. The hyperparameters of PSO are chosen as the dimension of 6 representing the six parameters to be optimized: R_0, R_1, R_2, C_1, CPE and α_3, acceleration factor =0.1, minimum inertia weight 0.5, maximum inertia weight =1, population size =50 and number of generations=500. The parameters are optimized using (7) for each 10% decay between 0 and 100% SOC inclusive storing 11 values for which parameters are linearly interpolated between input points. A comparison of the output voltages from the FOM and IOM with the experimental terminal voltage in the time domain is given in Fig. 6 where the zoomed view clearly shows that the FOM mimics the experimental voltage better than the IOM.

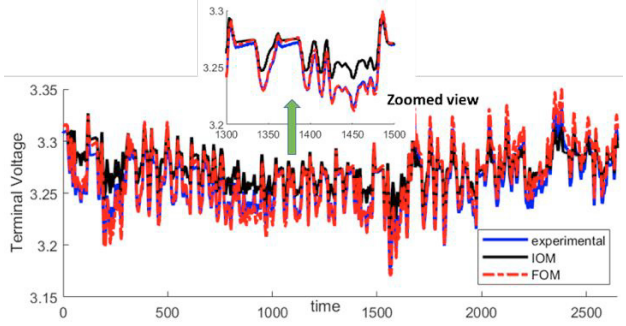

Fig. 6. Comparison of the proposed FOM, IOM and experimental terminal voltages of the LFP battery

4.2 Step 2 of the framework: Nonlinear observer results

This subsection implements the second step of the FO framework discussed in Section 3 that involves the nonlinear observer design. The initial condition of the SOC of the LFP battery is 70% and the that of the FO nonlinear estimator is 60%. An asymmetric charging discharging current profile as in Fig. 5 is fed as input to the battery and the estimator. The actual SOC is obtained by Coulomb counting through high fidelity measurements of the input current which are integrated with respect to time. Figure 7 shows that the estimated SOC despite being initialized from a different value, converges effectively to the actual SOC obtained from the battery experiment, thus, successfully estimating it. The steady state error of 0.6% is obtained between the experimental and simulated results.

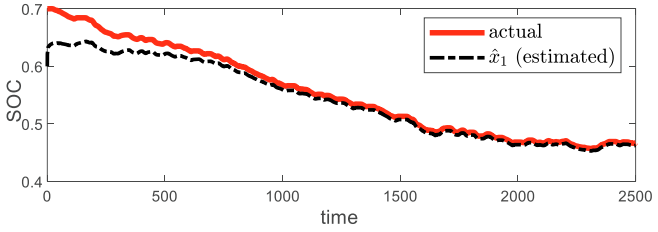

Fig. 7 Actual and estimated SOC in charging- discharging mode of the LFP battery

The driving speed profile of an EV is transformed to a demand power profile which in turn is changed into current by an energy management module to be fed to the battery. For comparison with existing literature, derivation of existing FOMs of LFP in (Rao et al., 2021) is not validated experimentally and the estimation technique being a low gain linear observer may not guarantee convergence. In our proposed work where we take care of nonlinear dependencies of parameters versus SOC, we obtain an error of 0.6% between the experimental and estimated results. The error is less than the 0.8% and 0.91% errors obtained in the FO approaches in (Li et al., 2023 and Wei et al., 2022), respectively. Thus, our proposed method being an SOC dependent model can closely relate to the physical system in a practical scenario and provide improved estimation results with faster convergence.

Acknowledgement: M. Borah in this work is supported by Fulbright fellowship.

5. CONCLUSIONS

Efficient operation of an EV depends on high reliability of accurate estimation of SOC which in turn depends on the accurate modelling that closely captures the underlying energy storage dynamics. This paper presents a two-step framework of fractional order dynamics applied to SOC estimation of $LiFePO_4$ batteries, the first being the proposal of a FO model of the battery where each circuit element in addition to the FO operator has nonlinear functionalities dependent on SOC. Practically, the FO parameter, α captures the dynamics of the non-integral relationships of voltage and current in the low frequency region and thereby provides an improved representation of the battery solid phase diffusion dynamics as the charge-discharge cylces progress. The second step of the framework presents the design of the nonlinear observer in the FO sense to estimate the SOC. The gain matrix is selected such that the error dynamics satisfy the fractional-order Lyapunov stability analysis and converge to zero. In practical scenarios, the proposed nonlinear fractional-order dynamical framework for precise estimation of SOC can be applied to attain an improved, sustainable, resilient, and efficient battery management system in smart cities applications, provide exact

driving range in electric vehicles, reduce maintenance cost and safety risks, enable fault diagnosis, and save energy.

The limitation of the proposed model is that the FO operator captures the dynamics in the low frequency region of the battery Nyquist curve. The future scope of this work is to use the FO operator as a function of SOC to model and understand the dynamics in the mid frequency region as well. Another direction of future scope is to study the FOM of the battery under the effects of hysteresis and temperature.

REFERENCES

Adhikary, A., Sen, P., Sen, S. *et al.* (2016). Design and Performance Study of Dynamic Fractors in Any of the Four Quadrants. *Circuits Syst Signal Process* vol. **35**, pp. 1909–1932.

Aguila-Camacho, N., Duarte-Mermoud, M. A., Gallegos, J. A. (2014). Lyapunov functions for fractional order systems. *Commun Nonlinear Sci Numer Simulat,* vol. 19*,* pp. 2951–2957.

Borah, M., Gayan, A., Sharma, J.S. *et al.* (2022) Is fractional-order chaos theory the new tool to model chaotic pandemics as Covid-19?. *Nonlinear Dyn* vol. 109, pp. 1187–1215.

Borah, M., & Roy, B. K. (2017). Fractional-order systems with diverse dynamical behaviour and their switching-parameter hybrid-synchronisation. *The European Physical Journal Special Topics*, vol. 226, 3747-3773.

Borah, M., & Roy, B. K. (2018, June). A novel multi-wing fractional-order chaotic system, its synchronisation control and application in secure communication. In *2018 2nd International Conference on Power, Energy and Environment: Towards Smart Technology (ICEPE)* (pp. 1-6). IEEE.

Chen, L., Yu, W., Cheng, G., & Wang, J. (2023). State-of-charge estimation of lithium-ion batteries based on fractional-order modeling and adaptive square-root cubature Kalman filter. *Energy*, vol. 271, 127007.

Dey, S., and Ayalew, B. (2014). Nonlinear Observer Designs for State-of-Charge Estimation of Lithium-ion Batteries. *American Control Conference (ACC)* June 4-6, 2014. Portland, Oregon, USA, pp. 248-253.

Dey, S., Ayalew, B. and Pisu, P. (2015). Nonlinear Robust Observers for State-of-Charge Estimation of Lithium-Ion Cells Based on a Reduced Electrochemical Model. *IEEE Transactions on Control Systems Technology*, vol. 23, no. 5, pp. 1935-1942.

Duan, Y., Chen, N., Chang, L., Ni, Y. , Kumar S. V. N. S. , and Zhang, P. (2022). CAPSO: Chaos Adaptive Particle Swarm Optimization Algorithm, in *IEEE Access*, vol. 10, pp. 29393-29405.

Klender, J. (2021). Tesla switches standard range vehicles to LFP batteries chemistry. *Teslarati*, https://www.teslarati.com/tesla-switches-standard-range-vehicles-to-lfp-battery-chemistry/

Li, M., Wang, L., Wang, Y., Chen, X. and Chen, Z. (2023). A Framework for States Co-Estimation of Hybrid Energy Storage Systems Based on Fractional-Order Theory. in *IEEE Journal of Emerging and Selected Topics in Power Electronics*, vol. 11, pp. 224-233.

Liu, M., Xu, J., Jiang, Y., & Mei, X. (2023). Multi-dimensional features based data-driven state of charge estimation method for LiFePO4 batteries. Energy, 127407.

Monje, C. A., Chen, Y., Vinagre, B. M., Xue, D., Feliu, V., (2010). Fractional-order Systems and Controls, *Springer-Verlag London Limited.* pp. 36-45.

Nasser-Eddine, A., Huard, B., Gabano, J.D. and Poinot, T. (2019). A two steps method for electrochemical impedance modeling using fractional order system in time and frequency domains. *Control Eng. Pract*., vol. 86, pp. 96–104.

Rao, K. D., Chander, A. H., & Ghosh, S. (2021). Robust observer design for mitigating the impact of unknown disturbances on state of charge estimation of lithium iron phosphate batteries using fractional calculus. *IEEE Transactions on Vehicular Technology*, *70*(4), pp. 3218-3231.

Tian, D. (2017). Particle swarm optimization with chaos-based initialization for numerical optimization. *Intelligent Automation & Soft Computing*, pp. 1-12.

Volta foundation, (2021) Battery report 2021, https://www.volta.foundation/annual-battery-report#

Wang, B., Liu, Z., Li, S. E., Moura, S. J. and Peng, H. (2017). State-of-Charge Estimation for Lithium-Ion Batteries Based on a Nonlinear Fractional Model, *IEEE Transactions on Control Systems Technology*, vol. 25, pp. 3-11.

Wang, Y., Chen, Y. and Liao, X. (2019). State-of-art survey of fractional order modeling and estimation methods for lithium-ion batteries. *Fractional Calculus and Applied Analysis*, *22*(6), 1449-1479.

Wang, Y., Han, X., Guo, D., Lu, L., Chen, Y. and Ouyang, M. (2022). Physics-Informed Recurrent Neural Networks with Fractional-Order Constraints for the State Estimation of Lithium-Ion Batteries. *Batteries*.; vol. 10, pp.148.

Wei, Y., & Ling, L. (2022). State-of-charge estimation for lithium-ion batteries based on temperature-based fractional-order model and dual fractional-order kalman filter. *Ieee Access*, vol. 10, 37131-37148.

Yao, J., & Han, T. (2023). Data-driven lithium-ion batteries capacity estimation based on deep transfer learning using partial segment of charging/discharging data. Energy, 271, 127033.